The EJC component *Magoh* regulates proliferation and expansion of neural crest-derived melanocytes

Debra L. Silver [a,b,*], Karen E. Leeds [a], Hun-Way Hwang [a], Emily E. Miller [b], William J. Pavan [a,**]

[a] Genetic Disease Research Branch, National Human Genome Research Institute, Bethesda, MD 20892, USA
[b] Department of Molecular Genetics and Microbiology, Duke University Medical Center, Durham, NC 27710, USA

ABSTRACT

Melanoblasts are a population of neural crest-derived cells that generate the pigment-producing cells of our body. Defective melanoblast development and function underlies many disorders including Waardenburg syndrome and melanoma. Understanding the genetic regulation of melanoblast development will help elucidate the etiology of these and other neurocristopathies. Here we demonstrate that *Magoh*, a component of the exon junction complex, is required for normal melanoblast development. *Magoh* haploinsufficient mice are hypopigmented and exhibit robust genetic interactions with the transcription factor, *Sox10*. These phenotypes are caused by a marked reduction in melanoblast number beginning at mid-embryogenesis. Strikingly, while *Magoh* haploinsufficiency severely reduces epidermal melanoblasts, it does not significantly affect the number of dermal melanoblasts. These data indicate *Magoh* impacts melanoblast development by disproportionately affecting expansion of epidermal melanoblast populations. We probed the cellular basis for melanoblast reduction and discovered that *Magoh* mutant melanoblasts do not undergo increased apoptosis, but instead are arrested in mitosis. Mitotic arrest is evident in both *Magoh* haploinsufficient embryos and in *Magoh* siRNA treated melanoma cell lines. Together our findings indicate that *Magoh*-regulated proliferation of melanoblasts in the dermis may be critical for production of epidermally-bound melanoblasts. Our results point to a central role for *Magoh* in melanocyte development.

© 2013 Elsevier Inc. All rights reserved.

Introduction

Melanocytes are specialized pigment-producing cells in vertebrates derived from the multipotent embryonic neural crest (Serbedzija et al., 1992, 1994). Melanocytes located in the integument generate melanin pigment that is responsible in mammals for coloration in skin and hair, and protection from solar UV radiation (Miyamura et al., 2007). Defects in melanocyte development and/or function are associated with multiple diseases including albinism, Waardenburg syndrome, and piebaldism (Harris et al., 2010). Additionally, malignant transformation of melanocytes causes melanoma, an extremely aggressive cancer that poses a significant health problem (Rigel, 2010). Thus, from both a developmental and disease standpoint, there is a need to understand the genes that regulate melanoblast function. In particular, the genes that are important for melanocyte proliferation

are thought to play a critical role in diseases of melanocytes, including melanoma.

Melanoblasts develop from the neural crest coincident with neural tube closure, which in mice occurs between embryonic (E) day 8.5 and 9.5 (Cable et al., 1995; Erickson et al., 1992; Larue et al., 2012; Silver et al., 2006). They migrate dorso-laterally relative to the neural tube through the prospective dermis. Between E9.5 and E13.5, they undergo dramatic expansion in their population, rapidly proliferating and suppressing apoptosis. Between E11.5 and E15.5, a subset of melanoblasts migrates from the dermis into the epidermis and hair follicles, where they eventually produce melanin (Luciani et al., 2011). The relationship between dermal and epidermal melanoblasts was recently hypothesized to be dependent upon precise cell divisions. Luciani et al. proposed a model in which dermal melanoblasts undergo asymmetric cell divisions to generate two populations: dermally retained melanoblasts and dermal melanoblasts that migrate into the epidermis (Luciani et al., 2011). This raises the interesting possibility that expansion of melanoblasts in the dermis play a critical role in the production of epidermal-bound melanoblasts.

In an effort to identify new genes critical for coordinated melanocyte development, we recently carried out an N-ethyl-N-nitrosourea (ENU) mutagenesis screen in mice. The screen was

---

* Corresponding author at: Department of Molecular Genetics and Microbiology, Duke University Medical Center, Durham, NC 27710, USA. Fax +1 919 684 2790.
** Corresponding author at: Genetic Disease Research Branch, National Human Genome Research Institute, Bethesda, MD 20892, USA.
E-mail addresses: debra.silver@duke.edu (D.L. Silver), bpavan@nhgri.nih.gov (W.J. Pavan).

designed to identify alleles that exacerbate the hypopigmentation associated with haploinsufficiency for *Sox10*, a transcription factor essential for the development of neural crest-derived melanocytes and glia and for melanoma progression (Harris et al., 2010; Matera et al., 2008; Prasad et al., 2011; Southard-Smith et al., 1998). One novel hypopigmentation mutant identified from this screen was *Mos2* (*modifier of Sox10 spotting 2*).

We previously used positional cloning to map the *Mos2* mutation to *Magoh* (Silver et al., 2010). *Magoh* encodes a component of the core exon junction complex (EJC). The EJC is an assembly of proteins that binds to mRNA during splicing, subsequently promoting aspects of mRNA metabolism, including mRNA splicing, localization, mRNA translation, and nonsense-mediated decay (Ashton-Beaucage et al., 2010; Le Hir and Andersen, 2008; Michelle et al., 2012; Nott et al., 2004; Palacios et al., 2004). We previously demonstrated that *Magoh* haploinsufficiency causes reduced body and brain size, due to defects in neural progenitor division and altered neuron production (Silver et al., 2010). However these analyses did not elucidate why *Magoh* haploinsufficiency causes hypopigmentation. In this study we have used the *Magoh^{Mos2/+}* mouse model to define a critical role for *Magoh* in melanoblast expansion.

Materials and methods

Mouse genetics and husbandry

All mouse lines were maintained on a C57BL/6J background. The *Magoh^{Mos2/+}* and *Sox10^{LacZ/+}* lines were genotyped as previously described (Matera et al., 2008; Silver et al., 2010). *Dct*-LacZ mice were used as previously described (Silver et al., 2008). All of the mice described were bred and housed in an NHGRI animal facility according to NIH guidelines. Animal care was done in accordance with NHGRI institutional standards and was approved by the Institutional Animal Care and Use Committee, NHGRI, and NIH Institutional Review Board.

Whole mount staining

β-galactosidase activity staining was performed as previously described (Silver et al., 2008). In situ hybridization was performed using *Dct* or *Pmel17* probes, as previously described (Silver et al., 2008). Images of whole mount embryos were taken using a digital camera mounted on a Leica M125 Dissecting microscope.

Tissue sections staining

β-galactosidase-stained embryos were embedded in paraffin and 5 μM sections were made. Paraffin was removed using a series of Xylene washes and sections were counterstained with hematoxylin and eosin staining. For immunofluorescence, frozen sections were prepared from embryos fixed overnight in 4% paraformaldehyde, washed in PBS, and placed in 10% and 20% sucrose solutions overnight. 20 μm sections were prepared through the trunk in coronal orientation. The following antibodies were used at 1:200: mouse anti-β-galactosidase (Promega, Madison, WI), rabbit anti-cleaved Caspase-3 (Cell Signaling, Danvers, MA), rabbit anti-phospho-Histone H3 (Upstate Biotechnology, Temecula, CA), and anti-mouse and anti-rabbit FITC-conjugated and rhodamine-conjugated secondary antibodies (Invitrogen, CA). Staining was performed using the MOM kit and Vectashield mount with DAPI (Vector Labs). For images of mouse skin, skins were peeled from embryos, and flattened with a coverslip. Images of tissue sections were taken using a Zeiss Axioskop2 microscope with IPLab imaging software.

Quantitation of whole mount embryos and tissue sections

Quantitation of melanoblasts in whole mount in situ hybridizations was performed as previously described (Loftus et al., 2009). Briefly, melanoblast density was measured in several pre-defined regions, as shown in Fig. 3E, and as follows: Region A contains the melanoblasts found in the crease between the telencephalon and nasal process, extending towards the eye; Region C contains the area between the caudal boundary line from the eye to the mid-hindbrain in region B and a parallel line immediately anterior to the otic vesicle; Region E contains the melanoblast population lateral to the forelimb area; and Region F contains the melanoblasts present in the trunk as defined by the post-axial (caudal) side of the forelimb bud, throughout the trunk, up to the preaxial (anterior) side of the hindlimb bud. Quantitation was then performed using the following scale: 0=no melanoblasts; 1− < 12 melanoblasts within the region; 2=moderate number of melanoblasts, sparsely distributed; 3=even, numerous melanoblasts; 4=dense overlapping melanoblasts.

Quantitation of total, epidermal, and dermal melanoblast number in 20 μm sections was calculated by measuring LacZ-positive melanoblast number per section. The epidermis was defined morphologically by a layer of 2–3 nuclei deep above the basal membrane. Melanoblasts below the basal membrane were classified as dermal. At least 10 sections/embryo were measured to give an average value for each embryo. At least 3 embryos were quantified per genotype and averaged to give the values graphed in Fig. 5 and Supplementary Fig. 2. Quantitation of the apoptotic index and mitotic index per section were calculated using cleaved caspase-3- (CC3) or phospho-histone H3- (PH3) positive melanoblasts, as previously described, for at least 3 embryos/genotype and for at least 10 sections/embryo (Silver et al., 2008). *P* values were calculated using a student's *t*-test.

Cell culture analysis

ISE06 human melanoma cell-line were transfected with *Magoh* or control siRNAs. Cells were harvested for lysates or fixed in ethanol overnight for cell-cycle analysis 48 h after transfection. DNA content of fixed cells was measured by flow cytometry with propidium iodide staining. Western blots were performed to determine the efficiency of *Magoh* knockdown. For analysis of MEF growth, MEFs were generated from E14.5 littermate embryos as previously described (Silver et al., 2010). MEFs were cultured for two passages and the third passage of MEFs were used for analysis. Equal numbers of MEFs (100,000 cells) were plated at day 0 and then counted after 48 h in culture manually with a hemocytometer. For the control two independent MEF lines were averaged for +/+;*Tg-BAC* and for the mutant four independent MEF lines were averaged.

Quantitative RT-PCR

Gene expression was measured in primary human melanocytes and human and mouse cell lines using the Taqman real-time PCR gene expression assays: *Magoh* (Mm00487546_m1) and *Magoh* (Hs00830672_s1) from Applied Biosystems. The expression in each sample was normalized to *Gapdh* and conditions were used as previously described (Silver et al., 2010). For analysis of *MAGOH* expression in human melanoma cells the comparative Ct approach was used. For analysis of *Magoh* expression in primary melanocytes and melan-A cells, expression was generated relative to a standard curve.

Results

Haploinsufficiency for Magoh results in dorsal and ventral hypopigmentation

To first assess the role of *Magoh* in establishment of pigmentation, we performed a detailed evaluation of the coat color phenotype in *Magoh*$^{Mos2/+}$ adult mice. The hypopigmentation phenotype was 100% penetrant, as all *Magoh*$^{Mos2/+}$ mice exhibited ventral hypopigmentation ($n=42$ mice) (Fig. 1). We examined 19 *Magoh*$^{Mos2/+}$ mice in more detail (Table 1). Of these, 16% ($n=3$) exhibited hypopigmentation only on their ventrum, evident as small white spots such as exemplified in Fig. 1B. 68% ($n=13$) of *Magoh*$^{Mos2/+}$ mice exhibited more extensive hypopigmentation, apparent on both ventral and dorsal surfaces (Fig. 1A). In these mice, the ventral spot was quite large, extending between the forelimb and hindlimb regions while the dorsal spot was evident in a belt-like pattern at the midline of the torso. In the remaining *Magoh*$^{Mos2/+}$ mice, the area of dorsal hypopigmentation was noticeably larger and extended more laterally (16%, $n=3$). Strikingly, in 84% of *Magoh*$^{Mos2/+}$ mice examined ($n=16$), the ventrum showed white spotting surrounding a narrow, band-like pattern of pigmentation present in the midline (dubbed "oak tree") (Fig. 1A,B, lower panels). In these mice the oak tree was always more prominent in the posterior of the ventrum than the anterior. The hypopigmentation and oak tree pattern were observed in the *Magoh*^{Mos2} allele, as well as in two independent alleles generated from gene traps, *Magoh*$^{GT27/+}$ and *Magoh*$^{GT51/+}$ (Fig. 1B) (Silver et al., 2010). While the oak tree pattern has not previously been observed in other pigmentation mutants, the ventral spotting and belting are similar to those seen in other mouse pigment mutants, including *Adamts20/Belted*, *Pax3/Splotch*, and *Ednrb/Piebald* (http://www.informatics.jax.org) (Baxter et al., 2010; Silver et al., 2008). Together this analysis indicates that *Magoh* influences pigmentation on both dorsal and ventral regions of the adult mouse.

Next we assessed pigmentation in mice haploinsufficient for both *Sox10* and *Magoh* (*Magoh*$^{Mos2/+}$;*Sox10*$^{LacZ/+}$). The *Magoh*$^{Mos2/+}$ phenotype was originally identified from a genetic interaction screen with *Sox10*, in which *Magoh*$^{Mos2/+}$;*Sox10*$^{LacZ/+}$ mice exhibited increased hypopigmentation as compared to *Sox10*$^{LacZ/+}$ mice (Matera et al., 2008). The initial screen was performed on a mixed Balb/cJ and C57Bl/6J genetic background. Therefore we tested if *Magoh* and *Sox10* would genetically interact on an inbred C57Bl/6J

background. We discovered that *Magoh*$^{Mos2/+}$;*Sox10*$^{LacZ/+}$ mice on a C57Bl/6J background exhibited genetic interactions similar to those seen on a mixed background (Fig. 1C) (Matera et al., 2008). This indicates that the inbred C57Bl/6J background introduced no new modifier effects. We next analyzed the pigmentation pattern of *Magoh*$^{Mos2/+}$;*Sox10*$^{LacZ/+}$ mice on the C57Bl/6J background in more detail. *Magoh*$^{Mos2/+}$;*Sox10*$^{LacZ/+}$ mice showed a much larger region of ventral and dorsal hypopigmentation than that seen in *Magoh*$^{Mos2/+}$ alone (compare Fig. 1C to A, B). Strikingly, while the extent of hypopigmentation is synergistically increased in *Magoh*$^{Mos2/+}$;*Sox10*$^{LacZ/+}$ mice, these mice show no evidence of the pigmented oak tree pattern present in *Magoh*$^{Mos2/+}$ mice (100%, $n=4$). This indicates that the *Sox10* mutation is epistatic to *Magoh* for the oak-tree phenotype.

Sox10-positive melanoblast development is impaired in Magoh$^{Mos2/+}$ embryos

The belly spot phenotype observed in *Magoh*$^{Mos2/+}$ and *Magoh*$^{Mos2/+}$;*Sox10*$^{LacZ/+}$ mutant mice indicated that *Magoh* might affect pigmentation by regulating melanoblast development. To test this potential function for *Magoh*, we compared melanoblast development in *Sox10*$^{LacZ/+}$ and *Magoh*$^{Mos2/+}$;*Sox10*$^{LacZ/+}$ embryos at developmental time points spanning from the initial to late stages of melanoblast development (E11.5–E16.5) (Fig. 2). The *Sox10*$^{LacZ/+}$ allele drives *LacZ* expression in melanoblasts as well as other neural crest derivatives during embryonic development (Britsch et al., 2001), thus allowing us to use β-galactosidase activity to mark the *Sox10*-expressing cells in whole embryos. At E11.5, there was no notable difference in *Sox10*-positive melanoblasts in a *Magoh*$^{Mos2/+}$ background (Fig. 2A, B). However beginning at E12.5 we observed a striking reduction in *Sox10*-positive cells in the *Magoh*$^{Mos2/+}$;*Sox10*$^{LacZ/+}$ embryos (Fig. 2C–F). Melanoblasts were reduced in the trunk laterally between both limbs, but not in the tail

Table 1
Distribution of mice with hypopigmentation patterns.

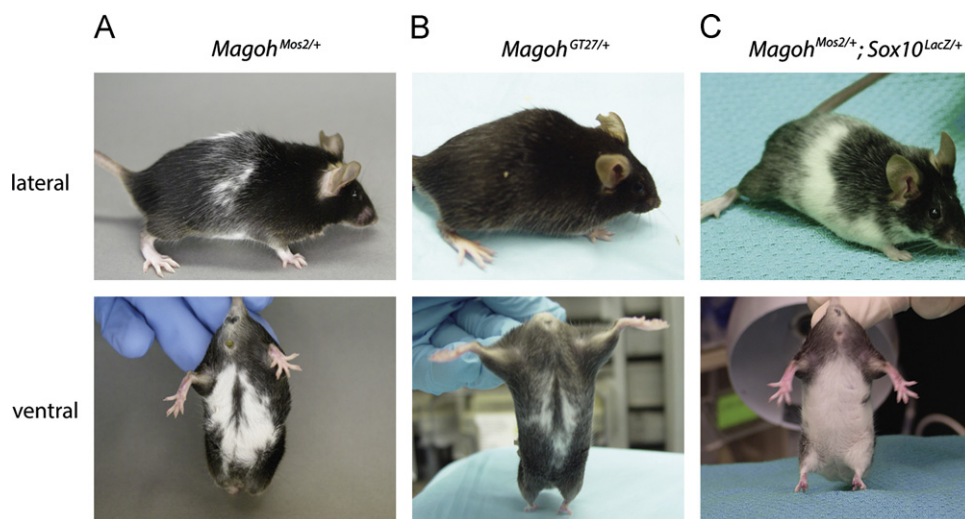| Hypopigmentation phenotype	Number mice	% Of mice
Small ventral spot	3	16
Large ventral spot AND Small dorsal spot	13	68
Large ventral spot AND Dorsal belt	3	16

Fig. 1. *Magoh* haploinsufficient mice exhibit hypopigmentation. (A–C) Lateral and ventral views of mice of the following genotypes: (A) *Magoh*$^{Mos2/+}$, (B) *Magoh*$^{GT27/+}$, (C) *Magoh*$^{Mos2/+}$; *Sox10*$^{LacZ/+}$.
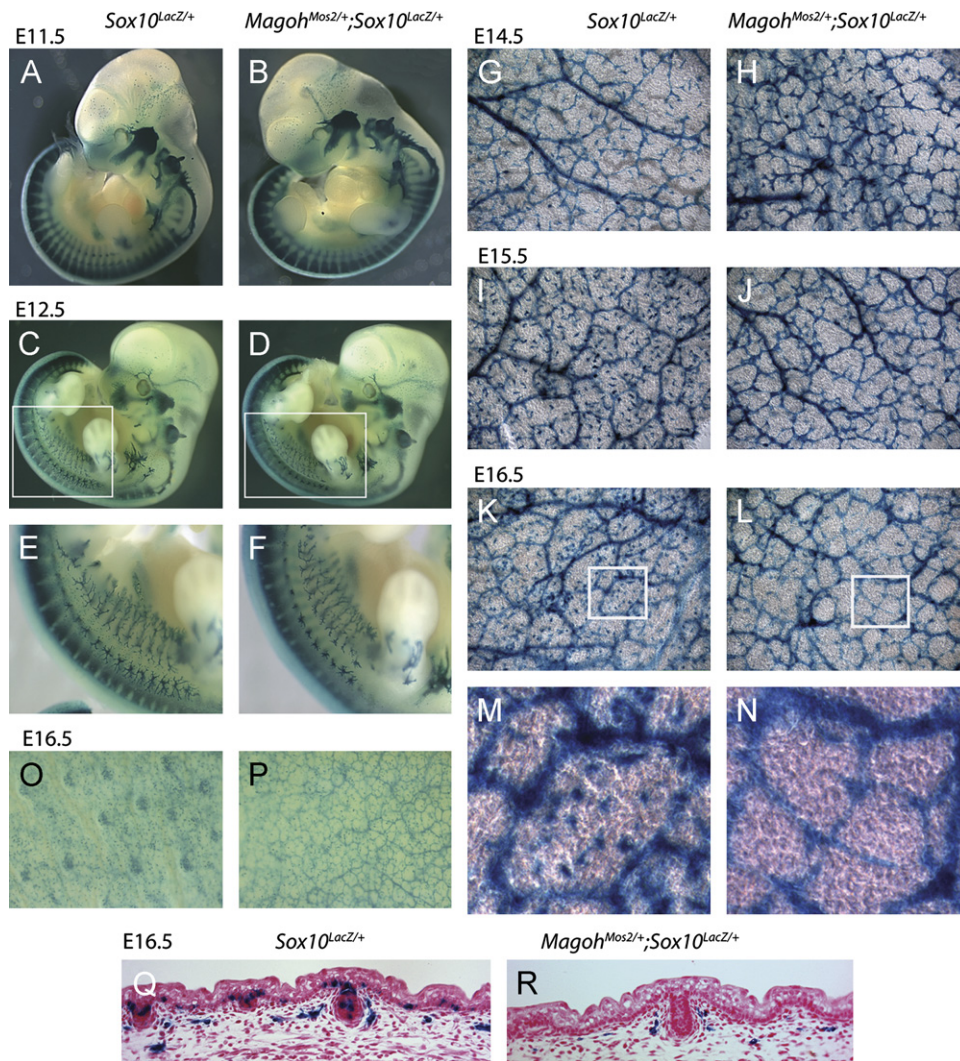
Fig. 2. Analyses of melanoblast development in $Magoh^{Mos2/+}$;$Sox10^{LacZ/+}$ embryos show that $Magoh$ genetically interacts with $Sox10$. (A–F) Images of β-galactosidase-stained whole mount $Sox10^{LacZ/+}$ (A,C,E) and $Magoh^{Mos2/+}$;$Sox10^{LacZ/+}$ embryos (B,D,F) at E11.5 (A,B) and E12.5 (C–F). (E,F) High magnification view of region outlined in boxes in (C,D). (G–N) Images of the underside of skin from β-galactosidase-stained $Sox10^{LacZ/+}$ (G,I,K,M) and $Magoh^{Mos2/+}$;$Sox10^{LacZ/+}$ embryos (H,J,L,N) at E14.5 (G,H), E15.5 (I,J), and E16.5 (K–N). (M,N) High magnification view of region outlined in boxes in (K,L). (O,P) High magnification images of β-galactosidase-stained whole mount E16.5 $Sox10^{LacZ/+}$ and $Magoh^{Mos2/+}$; $Sox10^{LacZ/+}$ embryos. (Q,R) Paraffin sections of β-galactosidase-stained and H & E-stained integument from E16.5 $Sox10^{LacZ/+}$ and $Magoh^{Mos2/+}$;$Sox10^{LacZ/+}$ embryos. Note $Sox10^{LacZ/+}$ shows expression in both melanoblasts (of the dermis and epidermis) as well as in the peripheral nervous system.

or head regions. This phenotype persisted in E13.5, E14.5, E15.5 and E16.5 embryos (Supplementary Fig. 1). Analysis of the underside of the embryonic skin provided additional evidence that the $Sox10$-positive melanocytes in the integument were significantly reduced between E14.5 and E16.5 (Fig. 2G–N). These data collectively indicate that beginning at E12.5, melanoblasts are reduced in $Magoh^{Mos2/+}$;$Sox10^{LacZ/+}$ embryos.

At E16.5, melanoblasts normally have begun to migrate into hair follicles, as evidenced by large blue clusters marking the hair follicles of $Sox10^{LacZ/+}$ embryos (Fig. 2O) (Silver et al., 2006). However in the $Magoh^{Mos2/+}$;$Sox10^{LacZ/+}$ embryos, there was a dramatic reduction in these follicle-associated melanoblast clusters (Fig. 2P). Histological analysis of E15.5 and E16.5 skin sections revealed that $Sox10$-positive melanoblasts were absent from developing hair follicles and significantly reduced in the epidermis of $Magoh^{Mos2/+}$;$Sox10^{LacZ/+}$ embryos (Fig. 2Q,R, data not shown). We also observed some reduction in $Sox10$-positive neural crest derivatives in the dermis (evident by morphology). The reduction in hair follicle melanoblasts in $Magoh^{Mos2/+}$;$Sox10^{LacZ/+}$ embryos was not due to defective hair follicle formation as histological analysis indicated that hair follicles formed similarly

and properly in the age matched $Magoh^{Mos2/+}$;$Sox10^{LacZ/+}$ and $Sox10^{LacZ/+}$ embryos (Fig. 2Q,R). Together these data indicate that $Magoh$ is required for development of a proper number of $Sox10$-positive trunk melanoblasts, particularly in the epidermis.

Magoh is required for melanoblast development independent from the Sox10 mutation

Given that $Magoh$ haploinsufficient mice are hypopigmented in the absence of a $Sox10$ mutation, we hypothesized that the $Magoh$ mutation alone would also impair melanoblast development. To examine melanoblast development in $Magoh^{Mos2/+}$ embryos without the $Sox10^{LacZ/+}$ mutation, we performed in situ hybridization against the melanoblast gene, $Pmel17$, on whole mount E11.5 and E12.5 embryos (Baxter and Pavan, 2003). We observed no qualitative differences in melanoblasts between C57BL/6J (control) and $Magoh^{Mos2/+}$ embryos at either age (Fig. 3A–D). In situ hybridization at E12.5 against mRNA expression of another melanoblast marker, Dct, also showed similar results (data not shown). We quantified the distribution and number of $Pmel17$-positive melanoblasts in four regions of these
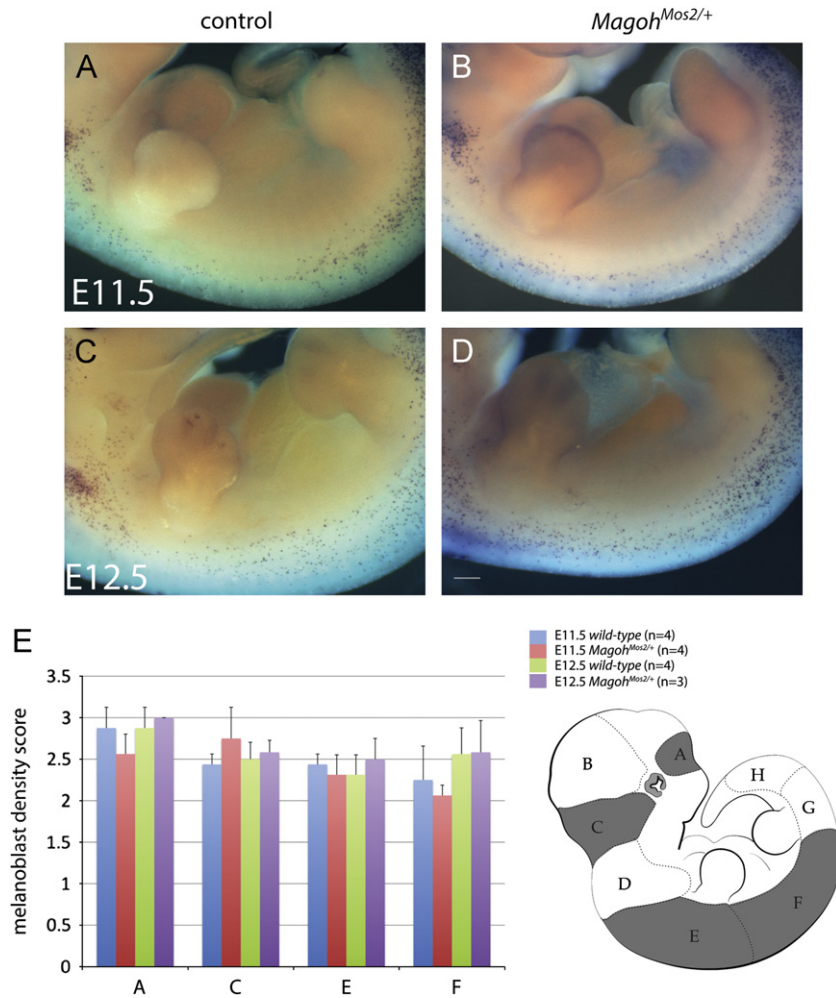
Fig. 3. *In situ* hybridization analyses show melanoblasts are distributed normally in E11.5 and E12.5 *Magoh*^{Mos2/+} embryos. (A–D) Images of whole mount *Pmel17* in situ hybridizations of *control* (A,C) and *Magoh*^{Mos2/+} (B,D) embryos at E11.5 (A,B), and E12.5 (C,D). (E) Quantitation of density of embryonic melanoblasts at E11.5 and E12.5 from specific anatomical regions, as indicated in schematic on right. A score was assigned as described in the materials and methods. Error bars=standard deviation. Note that there was no significant difference observed between control and mutants.

embryos using a quantitative approach previously described by our lab (Fig. 3E) (Loftus et al., 2009). This analysis also revealed no significant difference between control and *Magoh*^{Mos2/+} embryos at these early stages of melanoblast development (Fig. 3E).

We next evaluated melanoblast development in *Magoh*^{Mos2/+} embryos using a transgenic marker of melanoblasts, *Dct*-LacZ. Similar to the in situ hybridization results, E11.5 and E12.5 whole mount *Magoh*^{Mos2/+}; *Dct*-LacZ embryos showed no overt reduction in melanoblast distribution compared to *Dct*-LacZ (control) embryos (Fig. 4A–D and data not shown). Taken together, these data indicate that at E11.5 and E12.5, melanoblast number is relatively normal in *Magoh*^{Mos2/+} embryos. This result contrasts with the timing of defects in *Magoh*^{Mos2/+};*Sox10*^{LacZ/+} embryos, which are evident at E12.5.

We next evaluated melanoblast development in older E13.5 and E14.5 *Magoh*^{Mos2/+}; *Dct*-LacZ and control embryos to determine if there is a melanoblast defect at later stages. In control E13.5 embryos, melanoblasts are normally distributed laterally and throughout the head region (Fig. 4E,G) (Silver et al., 2006). However in E13.5 *Magoh*^{Mos2/+}; *Dct*-LacZ embryos, there was a noticeable reduction in *Dct*-LacZ positive melanoblasts in the lateral lumbar regions, and a slight reduction in the head (Fig. 4F,H). Similar differences between *Magoh*^{Mos2/+}; *Dct*-LacZ and control embryos were also evident at E14.5 (Fig. 4I–L). In E14.5 control embryos, melanoblasts are evenly distributed across

the length of the embryo, covering all surfaces except the ventrum adjacent to the umbilical cord (Fig. 4I,K, data not shown). However in E14.5 *Magoh*^{Mos2/+}; *Dct*-LacZ embryos, there was a marked reduction in melanoblasts in the trunk, with a large ventral area devoid of *Dct*-LacZ-positive cells (Fig. 4J). There was also a slight but noticeable reduction in the head (Fig. 4L). Of note, in the *Magoh*^{Mos2/+}; *Dct*-LacZ embryos there was no evidence of melanoblasts filling in the ventral region, where the "oak tree" was observed in adult mice (data not shown). Together these results indicate that *Magoh* haploinsufficiency causes a reduction in both trunk and head melanoblasts by E13.5. Because the *Magoh*^{Mos2/+};*Sox10*^{LacZ/+} phenotype was evident prior to this stage, our results indicate that one way the *Sox10* mutation exacerbates the melanoblast defect in *Magoh*^{Mos2+/} embryos is by affecting an earlier stage of melanoblast development.

Magoh haploinsufficiency results in striking changes in melanoblast number and location

To further elucidate how *Magoh* influences melanoblast development, we quantified melanoblast number and distribution in embryonic sections from *Magoh*^{Mos2/+}; *Dct*-LacZ and control embryos. Consistent with our analyses of whole mount embryos, the average number of melanoblasts/section at E12.5 was not significantly different between *Magoh*^{Mos2/+}; *Dct*-LacZ and control
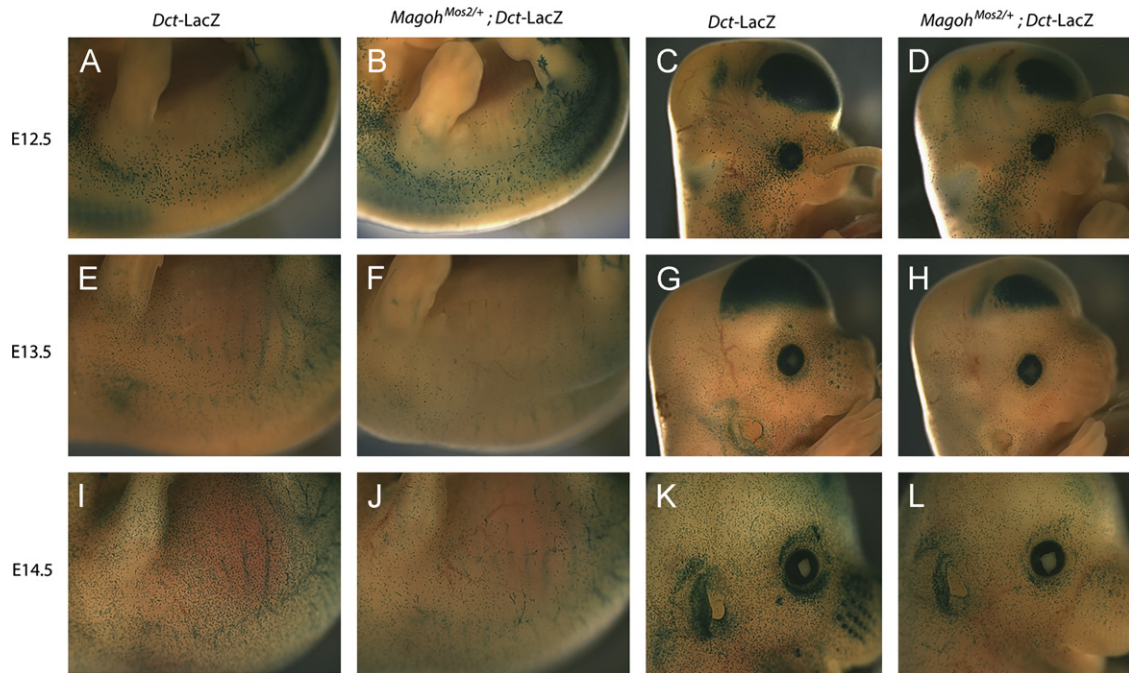
Fig. 4. *Magoh* distribution is defective in whole mount *Magoh*[Mos2/+] embryos at E13.5 and E14.5. (A–L) Images of β-galactosidase stained whole mount *Magoh*^{+/+}; *Dct-LacZ* (*Dct*-LacZ) (A,E,I,C,G,K) and *Magoh*[Mos2/+]; *Dct-LacZ* embryos (B,F,J,D,H,L) at E12.5 (A–D), E13.5 (E–H), and E14.5 (I–L).

embryos (average=21/section for both genotypes, $P=0.3902$) (Fig. 5A). In contrast, at E13.5 there was a 30% reduction in *Magoh*[Mos2/+]; *Dct*-LacZ melanoblasts compared to control (average=22/section versus 32/section respectively, $P<0.00001$) (Fig. 5A). At E14.5 this difference was even more pronounced, with an 80% reduction in *Magoh*[Mos2/+]; *Dct*-LacZ melanoblasts compared to control (average=27/section versus 70/section respectively, $P<0.00001$). These quantitative analyses reveal two important findings. First, differences in melanoblast numbers between control and *Magoh* mutants increased strikingly from E13.5 to E14.5 as development proceeded. Second, the average melanoblast number in *Magoh*[Mos2/+] embryos remained relatively constant from E13.5 to E14.5 while control melanoblasts increased in density over this time period.

To evaluate whether melanoblast distribution within the developing integument was altered in *Magoh*[Mos2/+] embryos, we quantified melanoblasts in dermal and epidermal layers of E13.5 and E14.5 sections from *Magoh*[Mos2/+]; *Dct*-LacZ and control embryos. There were no significant difference in the number of dermal melanoblasts of control and *Magoh*[Mos2/+]; *Dct*-LacZ E13.5 embryos (9 versus 9.4, respectively, $P=0.79$) or E14.5 embryos (9.2 versus 12.3, respectively, $P=0.24$) (Fig. 5B). In contrast, there were significantly more epidermal melanoblasts in control embryos compared to *Magoh*[Mos2/+]; *Dct*-LacZ embryos at both E13.5 and E14.5 (Fig. 5C). At E13.5 this difference was 23.9 melanoblasts/section versus 13.4 for control and *Magoh*[Mos2/+]; *Dct*-LacZ embryos, respectively ($P<0.00001$). This difference was even more pronounced at E14.5, when control embryos contained a five-fold higher epidermal melanoblast number than seen in *Magoh*[Mos2/+]; *Dct*-LacZ embryos (compare 64.5 versus 14.8 respectively, $P<0.00001$). Together these data indicate that *Magoh* exerts a major effect upon melanoblast development and is required to achieve normal epidermal melanoblast number.

Magoh haploinsufficiency does not affect melanoblast survival but does cause mitotic arrest

The melanoblast reduction is first evident in E13.5 *Magoh*[Mos2/+] embryos, which is a critical time point in melanoblast development

for expansion of the melanoblast population. At this stage melanoblasts expand in number by both rapid proliferation and by exerting pro-survival mechanisms (Mackenzie et al., 1997; Silver et al., 2006; Silver et al., 2008). We predicted *Magoh* haploinsufficiency could deplete melanoblasts by either of these mechanisms. To test this, we first we examined whether there was increased melanoblast apoptosis in *Magoh*[Mos2/+]; *Dct-LacZ* embryos, by calculating apoptotic indices in control and *Magoh*[Mos2/+]; *Dct-LacZ* embryos (see Fig. 5D, F–H). We measured melanoblast apoptosis in E12.5–E14.5 embryos because these ages span the observed melanoblast phenotype. At E12.5 there was no significant increase in the apoptotic index in control versus *Magoh*[Mos2/+]; *Dct-LacZ* embryos (0.72% versus 0.83%, respectively, $P=0.3437$) (Fig. 5D). This result is consistent with normal melanoblast number observed in *Magoh*[Mos2/+]; *Dct*-LacZ at this age. At E13.5, the apoptotic index was also not significantly different between control and *Magoh*[Mos2/+]; *Dct-LacZ* embryos (0.36 versus 1.1, respectively, $P=0.182$). Similar results were seen at E14.5, when the apoptotic index was 0.29 and 0.31 in control and *Magoh*[Mos2/+]; *Dct-LacZ* embryos, respectively ($P=0.9039$). Together these quantitative analyses indicate that the gross reduction in melanoblast number in *Magoh*[Mos2/+] embryos is not due to increased melanoblast apoptosis. This is in contrast to other mutants, such as *belted*, which exhibit loss of melanoblasts due to apoptosis (Silver et al., 2008).

We hypothesized that the reduced melanoblast number in *Magoh*[Mos2/+] embryos could be due to defects in melanoblast proliferation. Therefore we determined whether melanoblasts in E12.5–E14.5 *Magoh*[Mos2/+]; *Dct*-LacZ embryos underwent altered cell division by calculating average mitotic indices (Fig. 5E, H–J, Supplementary Fig. 2). In E12.5 control and *Magoh*[Mos2/+]; *Dct-LacZ* embryos, the average mitotic index was not significantly different (2.1 versus 2.27 respectively, $P=0.8098$; Supplementary Fig. 2). This result is consistent with the observation that melanoblast number in E12.5 *Magoh*[Mos2/+] embryos is normal (Fig. 5A). However, E13.5 *Magoh*[Mos2/+]; *Dct*-LacZ embryos showed a striking five-fold increase in mitotic index relative to control embryos (4.26 versus 0.93, respectively, $P=0.007$; Fig. 5H). This trend continued in E14.5 embryos, with a two-fold increase in the mitotic index of
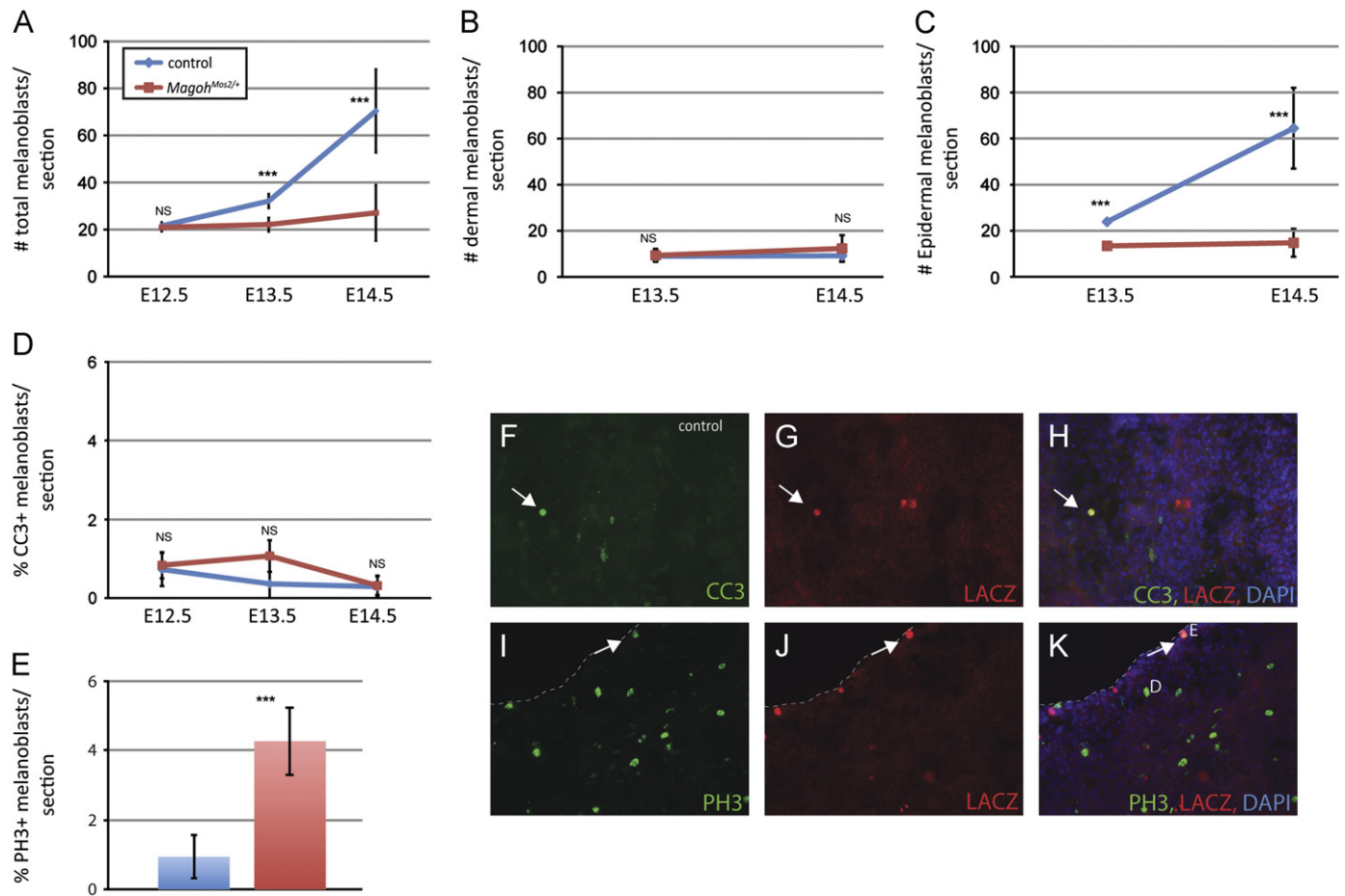
Fig. 5. Reduced melanoblast number and increased melanoblast proliferation in $Magoh^{Mos2/+}$ embryos. (A–C) Graphs showing average melanoblast number/section in $Magoh^{+/+}$; $Dct\text{-}LacZ$ (control) and $Magoh^{Mos2/+}$; Dct-LacZ at E12.5, E13.5, and E14.5, including: total number of melanoblasts (A), total number of dermal melanoblasts (B), and total number of epidermal melanoblasts (C). (D) Graph representing average percentage of total melanoblasts that are CC3-positive at E12.5, E13.5, and E14.5. (E) Graph representing average percentage of total melanoblasts that are PH3-positive at E13.5. For A–E, each graphed point represents the average value of 3 independent embryos, with each embryo value averaged from at least 10 sections. (F–K) Representative immunofluorescence images of coronal sections stained for LacZ (melanoblasts, red) and either CC3 (apoptotic cells, green) (F–H) or PH3 (mitotic cells, green) (I–K). DAPI (blue) shows nuclei, and arrows indicate examples of co-labeled cells in the dermis (F–H) and epidermis (H–J). Error bars=standard deviations. NS=not significant. ***, $P < 0.00001$. In (I–K) a dotted line denotes the edge of the skin, and D=dermal melanoblast and E=epidermal melanoblast. (For interpretation of the references to color in this figure legend, the reader is referred to the web version of this article.)

$Magoh^{Mos2/+}$ relative to control embryos, although this difference was not statistically significant (2.05 versus 1.26, respectively, $P=0.17$; Supplementary Fig. 2). Together these results indicate that $Magoh$ haploinsufficiency causes mitotic arrest and impairs melanoblast proliferation. In light of our finding that melanoblasts are significantly reduced in number at E13.5, we conclude that melanoblasts are depleted in large part due to failure to expand in number.

Reduced Magoh expression in melanocyte-derived cells causes G2/M mitotic arrest

To further examine how $Magoh$ influences melanoblast expansion, we used a cell culture model. We first measured $Magoh$ mRNA expression in different sources of melanocytes, including a mouse melanocyte cell line (melan-a), human primary melanocytes, and a panel of human melanocyte-derived cell lines (Supplementary Fig. 3). This analysis revealed that $Magoh$ is expressed in both primary and immortalized melanocyte-derived cell lines. We selected the melanoma cell line, ISE06 for functional siRNA analysis because this cell line is amelanocytic, making it possible to do propidium iodide staining and cell cycle analysis. Moreover, $Magoh$ is expressed at a moderate level in this cell line, making it feasible to knock-down its endogenous expression. Using siRNA knockdown of $Magoh$ in ISE06 cells,

we achieved a dramatic reduction in Magoh protein levels as compared to control cells (Fig. 6A). We then carried out FACs analyses of these cells to measure the DNA content and cell cycle stage (Fig. 6B). This analysis showed that the siRNA-mediated knockdown of $Magoh$ expression in the ISE06 cell line significantly increased the percentage of cells in G2/M ($Magoh$ siRNA=36%, scrambled siRNA=11%, untreated=12%). To determine if $Magoh$ haploinsufficiency impacted net cell number we quantified growth of $Magoh^{Mos2/+}$ mouse embryonic fibroblasts (MEFs, passage 3) in culture (Supplementary Fig. 4). We found that after 48 hours in culture, there were significantly fewer $Magoh^{Mos2/+}$ MEFs compared to control ($P < 0.0045$). This trend was also evident in passage 2 MEFs (data not shown). Taken together, these results indicate that reduced $Magoh$ expression causes mitotic arrest at G2/M and impacts cell number. These in vitro findings are consistent with the increased number of mitotic melanoblasts (PH3-positive) and with the net reduction in melanoblasts observed in $Magoh$ haploinsufficient embryos.

Discussion

In this paper, we demonstrate that $Magoh$ is an essential regulator of melanoblast development. $Magoh$ haploinsufficient
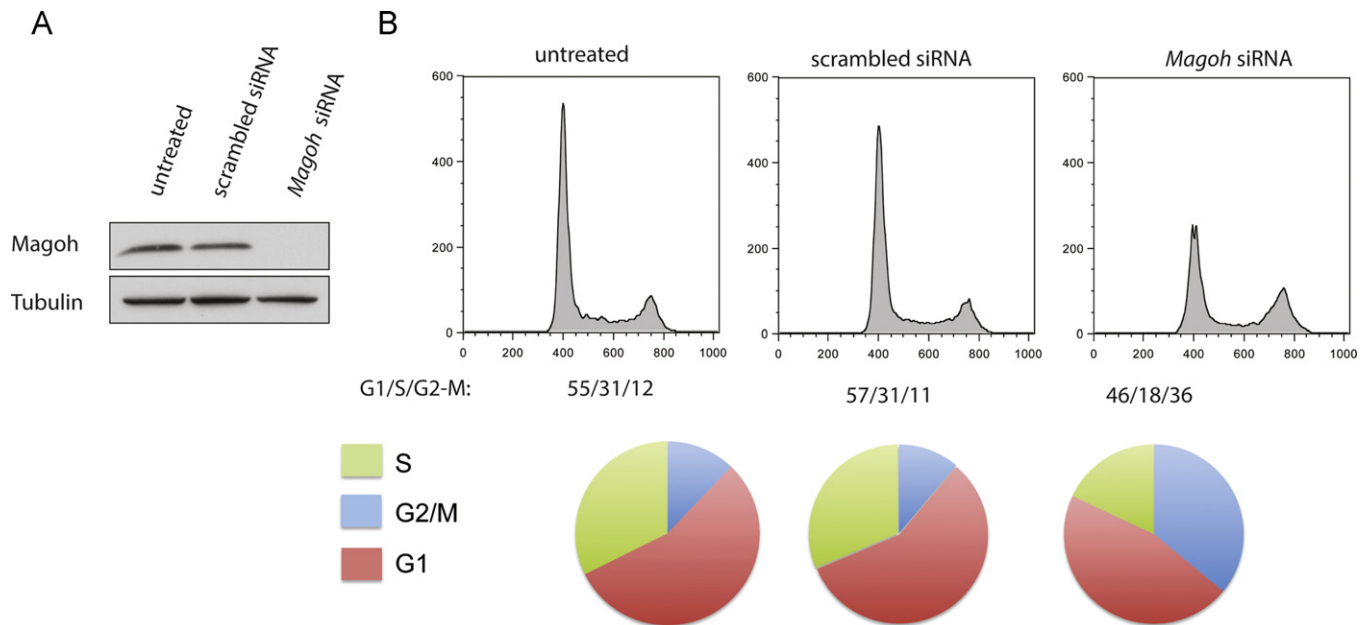
Fig. 6. *Magoh* depletion from a melanocyte-derived cell line causes G2/M arrest. (A) Immunoblots depicting Magoh and Tubulin protein expression in untreated, scrambled siRNA-treated, and *Magoh* siRNA-treated ISE06 cells. (B) Representative FACs profiles of untreated, scrambled siRNA-treated, and *Magoh* siRNA-treated ISE06 cells. Pie charts below each profile depict the proportion of cells in each phase of the cell cycle.

mice exhibit hypopigmentation due to dramatic reduction of melanoblast number during development. We find that this reduction is due to defects in melanoblast expansion that predominantly affect epidermal melanoblast populations. Moreover, the finding that *Magoh* depletion from a melanoma cell line causes cell cycle arrest indicates that influencing *Magoh* expression in melanomas could provide possible therapeutic options for these diseases. Together our study establishes *Magoh* as a new central regulator of melanocyte development, and thus has implications for our understanding of the genetic basis of melanocyte development disorders.

Magoh regulates melanoblast number

Normal melanoblast development requires the successful execution of multiple processes, including initial specification, migration, active cell survival, and extensive proliferation (Cable et al., 1995; Harris et al., 2010; Serbedzija et al., 1992; Silver et al., 2006). Through our analyses of melanoblast development, we pinpointed which of these processes are disrupted in *Magoh*$^{Mos2/+}$ embryos. Melanoblast specification and dorso-lateral migration from the neural tube is intact in *Magoh* mutants, as evidenced by the presence of *Dct*-positive and *Pmel17*-positive melanoblasts in the proper number and location in younger embryos. *Magoh* haploinsufficiency also does not disrupt melanoblast survival, as there was no increase in apoptotic indices of mutant melanoblasts. However, we found that *Magoh* is essential for proliferation of melanoblasts at a critical time in melanoblast expansion (Mackenzie et al., 1997). Hence, mitotic arrest of melanoblasts in *Magoh* mutants leads to an overall reduction in melanoblasts.

The reduced pattern of melanoblasts during embryogenesis is more dramatic then the adult hypopigmentation seen in *Magoh* haploinsufficient mice. We observed fewer melanoblasts throughout the head and trunk of *Magoh*$^{Mos2/+}$ embryos, however the mutant adults only exhibited trunk hypopigmentation. This is similar to other mutants such as *Adamts20*$^{bt/bt}$, in which there are reduced melanoblasts in the head of mutant embryos, but no cranial hypopigmentation in the adult (Silver et al., 2008). This difference is likely due to the fact that there are more

melanocytes in the head and thus a loss of melanocytes during embryogenesis does not affect overall pigmentation pattern in the head (Silver et al., 2008; Wilkie et al., 2002). It is also possible that the belly spot observed in *Magoh*$^{Mos2/+}$ adults may be caused by melanocytes that fail to produce or transfer melanin. Another difference between embryonic and adult *Magoh*$^{Mos2/+}$ phenotypes is the "oak-tree" pattern. In the adult *Magoh* haploinsufficient mice some pigmentation is evident within the ventral midline of the trunk, yet in *Magoh* haploinsufficient embryos we observed no evidence of melanoblasts populating the ventral trunk midline. We speculate that there may be a population of *Magoh*-independent melanoblasts that proliferates late in development within the ventral midline. Future studies using conditional temporal deletion of *Magoh* will be helpful to test this possibility.

While haploinsufficiency for *Magoh* reduces melanoblast number as early as E13.5, combined haploinsufficiency for both *Sox10* and *Magoh* reduces melanoblast number one day earlier in development. These phenotypes persist into adulthood, resulting in more extensive hypopigmentation in *Magoh*$^{Mos2/+}$;*Sox10*$^{LacZ/+}$ embryos relative to that seen in either *Sox10* or *Magoh* single mutants. This genetic interaction may be due to *Magoh* and *Sox10* acting in the same genetic pathway. Another explanation is that dosage of both genes is critical for melanoblast development but that each gene acts at a different time. Many genes known to regulate melanoblast development show dosage-dependent phenotypes as well as genetic interactions with other melanoblast genes (Silver et al., 2008). Indeed our results are compatible with both possibilities. For example, while *Sox10* haploinsufficiency is known to affect early melanoblast specification and survival, our study reveals that *Magoh* affects later melanoblast proliferation (Potterf et al., 2001; Southard-Smith et al., 1998). Further analyses will be helpful to elucidate the molecular relationship between *Sox10* and *Magoh* and whether *Magoh* also interacts with other melanoblast mutants.

Magoh regulates melanoblast expansion

We propose that *Magoh* enables melanoblasts to proceed through the cell cycle, and specifically through G2/M phases.

This is supported by our in vitro knockdown studies, in which *Magoh* deficient cells are arrested at G2/M and reduced in number, and our in vivo analyses of *Magoh* mutants, which have increased number of melanoblasts labeled with PH3, a marker for G2/M. Thus our data indicate that at E13.5 *Magoh* deficient melanoblasts are arrested in G2/M, and ultimately fail to expand, leading to a net reduction in melanoblasts at E13.5 and E14.5. At E14.5 the trend of more PH3 positive melanoblasts in *Magoh* haploinsufficient mutants continued, although it was not statistically significant. We speculate that at E13.5, melanoblasts may be especially sensitive to perturbations of the cell cycle, as other pigmentation mutants affect cell number at this age (Silver et al., 2008; Yoshida et al., 1996).

Our findings are consistent with a generalized role for *Magoh* in mitosis. siRNA knockdown of *Magoh* in HeLa cells causes G2/M arrest (Kittler et al., 2007; Silver et al., 2010). Moreover, similar to our in vitro findings with MEFs and melanocyte-derived cells, *Magoh* siRNA treated tsFT210 and FM3A cells show reduced proliferation in culture (Inaki et al., 2011). How might *Magoh* impact melanoblast division? We previously found that *Magoh* was required for chromosome segregation of *Magoh*^Mos2/+^ MEFs and for bipolar spindle formation of HeLa cells (Silver et al., 2010). Thus we predict that *Magoh* impacts melanoblast proliferation using similar cell biological mechanisms. At a molecular level, we postulate that *Magoh* may regulate expression of cyclin-dependent kinases (Cdks), as demonstrated by Inaki et al. (Inaki et al., 2011).

Our findings in melanocytes are consistent with a generalized role for *Magoh* in mitosis during development. In the developing cerebral cortex, we previously showed that *Magoh* regulates mitosis and cleavage planes of neural stem cells (Silver et al., 2010). *Magoh* haploinsufficient mice exhibit alterations in neurogenesis, with precocious production of neurons and loss of neural progenitors (Silver et al., 2010). Although ectopically produced neurons in the brain undergo cell death, such cell death is not apparent in *Magoh*-deficient melanoblasts. These differences could reflect cell-type specific responses to mitotic arrest. For example, melanoblasts may be more resilient in correcting DNA damage, in line with their ability to survive under DNA-damaging UV irradiation (Harris et al., 2010; Miyamura et al., 2007). Alternatively, it is also possible that apoptotic melanoblasts lost expression of melanoblast markers, making them undetectable in this study.

Magoh impacts epidermal melanoblasts

One surprising finding to come out of our study is that *Magoh* haploinsufficiency disproportionately affects epidermal melanoblasts. This is likely not due to a simple reduction in proliferation, because other mouse spotting mutants that affect melanoblast proliferation do not always show disproportionate effects upon epidermal and dermal populations. For example, Delmas and colleagues examined melanocyte development using mice with gain- and loss-of-function mutations in β-catenin (Luciani et al., 2011). They found that both types of alterations resulted in reduced numbers by affecting proliferation, however both the dermal and epidermal melanoblasts were reduced. They used results from this study to develop a mathematical model in which half of the progeny of dermal melanoblasts undergoing cell division give rise to cells that remain in the dermis, while the other half migrate from the dermis to the epidermis (Aylaj et al., 2011). This raises the interesting possibility that expansion of melanoblasts in the dermis plays a critical role in the production of epidermal-bound melanoblasts. Given the role of *Magoh* in specification of neurons in the brain, it is tempting to speculate that *Magoh* is similarly involved in regulating the fate of cells

generated from melanoblast divisions in the dermis. Thus the daughter cells derived from dermal melanoblasts in *Magoh* mutants could be compromised in their function and incapable of entering the epidermis. This cell fate mechanism could explain the extensive defect in epidermal melanoblasts seen in *Magoh* mutants.

An alternative explanation for the disproportionate reduction in epidermal melanoblasts is that *Magoh* influences Schwann cell precursors, which also generate melanocytes during development (Adameyko et al., 2009). Recent studies by Adameyko and colleagues described a population of developing melanoblasts arising from multipotent Schwann cell precursors located near cutaneous nerves that can first be identified between E12 and E13. This time period also marks the onset of the melanocyte phenotype in *Magoh* mutants. The Schwann cell precursors have been proposed to generate melanocytes that contribute mainly to the epidermal melanocytes while the dorsolaterally migrating cells contribute mainly to dermal populations. *Magoh* could function in at least two ways in Schwann cell precursors. First, *Magoh* could influence cell division of the Schwann cell precursors leading to subsequent reductions in the population of epidermal melanoblasts. Second, similar to *Magoh*'s role in cell fate specification in the brain, it could affect melanocyte specification by Schwann cell precursors, influencing whether their daughter cells generate progeny destined for Schwann cell or a melanocyte fates (Adameyko et al., 2009; Silver et al., 2010).

It is also striking to note that *Magoh* haploinsufficiency causes cell-specific phenotypes affecting primarily the brain and melanocytes. Because *Magoh* encodes a component of the exon junction complex (EJC) that mediates various aspects of mRNA metabolism, a reasonable a priori prediction would be that *Magoh* haploinsufficiency would cause more generalized phenotypes affecting multiple tissues. A possible reason for the specificity of *Magoh*^Mos2/+^ phenotypes is the expression of a redundant protein. Consistent with this, a homologous *Magoh2* gene is annotated in the genome (MGI.org), although its expression and function in melanocytes is unknown. Another explanation for the specificity of phenotypes is that melanoblasts and neurons are especially sensitive to dosage of *Magoh*. Consistent with this reasoning, when levels of *Magoh* and associated EJC components are extensively depleted via morpholinos in *Xenopus laevis*, more dramatic phenotypes are evident, including full-body paralysis and aberrant neuronal and cardiac development (Haremaki et al., 2010). In this study the authors also observed pigment cell loss with *Magoh* morpholinos, however they did not elucidate the cellular mechanism of this phenotype, nor how pigment cells are lost spatially and temporally. Given our findings, we predict that proliferation defects are at the root of many of the neural crest phenotypes observed in *Xenopus*. Taken together, these studies indicate a conserved role for the EJC in melanocyte and neural crest development.

Our results reveal that Magoh and EJC components are likely to play roles in the etiology of melanocyte disorders arising during development and in adulthood, including melanoma. Melanoma is caused by over-proliferation of melanocytes. It is intriguing to note that higher levels of *Magoh* are observed in some melanoma cell lines, and that *Magoh* depletion from these cells arrests causes mitotic arrest. This suggests the intriguing possibility that intervention of *Magoh* expression or function could be used as a potential therapeutic treatment of aggressive melanocyte cancers, including Melanoma. Thus our study may open up new areas of research probing how *Magoh* impacts melanoma progression and treatment.

Conclusions

This study is the first to dissect the in vivo requirement of *Magoh*, or any core exon junction complex (EJC) component in

neural crest development in mammals. Our study identifies an important regulator of melanocyte development. Moreover it additionally helps elucidate general cellular mechanisms guiding melanocyte development, and in particular the role of proliferation in expansion of melanocyte populations.

Acknowledgments

Appendix A. Supporting information

Supplementary data associated with this article can be found in the online version at http://dx.doi.org/10.1016/j.ydbio.2013.01.004.

References

Adameyko, I., Lallemend, F., Aquino, J.B., Pereira, J.A., Topilko, P., Muller, T., Fritz, N., Beljajeva, A., Mochii, M., Liste, I., Usoskin, D., Suter, U., Birchmeier, C., Ernfors, P., 2009. Schwann cell precursors from nerve innervation are a cellular origin of melanocytes in skin. Cell 139, 366–379.

Ashton-Beaucage, D., Udell, C.M., Lavoie, H., Baril, C., Lefrancois, M., Chagnon, P., Gendron, P., Caron-Lizotte, O., Bonneil, E., Thibault, P., Therrien, M., 2010. The exon junction complex controls the splicing of MAPK and other long intron-containing transcripts in Drosophila. Cell 143, 251–262.

Aylaj, B., Luciani, F., Delmas, V., Larue, L., De Vuyst, F., 2011. Melanoblast proliferation dynamics during mouse embryonic development. Modeling and validation. J. Theor. Biol. 276, 86–98.

Baxter, L.L., Moreland, R.T., Nguyen, A.D., Wolfsberg, T.G., Pavan, W.J., 2010. A curated online resource for SOX10 and pigment cell molecular genetic pathways. Database: J Biol. Databases Curation 2010, baq025.

Baxter, L.L., Pavan, W.J., 2003. Pmel17 expression is Mitf-dependent and reveals cranial melanoblast migration during murine development. Gene expression patterns: GEP 3, 703–707.

Britsch, S., Goerich, D.E., Riethmacher, D., Peirano, R.I., Rossner, M., Nave, K.A., Birchmeier, C., Wegner, M., 2001. The transcription factor Sox10 is a key regulator of peripheral glial development. Genes Dev. 15, 66–78.

Cable, J., Jackson, I.J., Steel, K.P., 1995. Mutations at the W locus affect survival of neural crest-derived melanocytes in the mouse. Mech. Dev. 50, 139–150.

Erickson, C.A., Duong, T.D., Tosney, K.W., 1992. Descriptive and experimental analysis of the dispersion of neural crest cells along the dorsolateral path and their entry into ectoderm in the chick embryo. Dev. Biol. 151, 251–272.

Haremaki, T., Sridharan, J., Dvora, S., Weinstein, D.C., 2010. Regulation of vertebrate embryogenesis by the exon junction complex core component Eif4a3. Dev. Dyn.: Off. Publ. Am. Assoc. Anat. 239, 1977–1987.

Harris, M.L., Baxter, L.L., Loftus, S.K., Pavan, W.J., 2010. Sox proteins in melanocyte development and melanoma. Pigm. Cell Melanoma Res. 23, 496–513.

Inaki, M., Kato, D., Utsugi, T., Onoda, F., Hanaoka, F., Murakami, Y., 2011. Genetic analyses using a mouse cell cycle mutant identifies magoh as a novel gene involved in Cdk regulation. Genes Cells: devoted to Mol Cell. Mech. 16, 166–178.

Kittler, R., Pelletier, L., Heninger, A.K., Slabicki, M., Theis, M., Miroslaw, L., Poser, I., Lawo, S., Grabner, H., Kozak, K., Wagner, J., Surendranath, V., Richter, C., Bowen, W., Jackson, A.L., Habermann, B., Hyman, A.A., Buchholz, F., 2007. Genome-scale RNAi profiling of cell division in human tissue culture cells. Nat. Cell Biol. 9, 1401–1412.

Larue, L., de Vuyst, F., Delmas, V., 2012. Modeling melanoblast development. Cell. Mol. Life Sci.: CMLS.

Le Hir, H., Andersen, G.R., 2008. Structural insights into the exon junction complex. Curr. Opin. Struct. Biol., 112–119.

Loftus, S.K., Baxter, L.L., Buac, K., Watkins-Chow, D.E., Larson, D.M., Pavan, W.J., 2009. Comparison of melanoblast expression patterns identifies distinct classes of genes. Pigm. Cell Melanoma Res. 22, 611–622.

Luciani, F., Champeval, D., Herbette, A., Denat, L., Aylaj, B., Martinozzi, S., Ballotti, R., Kemler, R., Goding, C.R., De Vuyst, F., Larue, L., Delmas, V., 2011. Biological and mathematical modeling of melanocyte development. Development 138, 3943–3954.

Mackenzie, M.A., Jordan, S.A., Budd, P.S., Jackson, I.J., 1997. Activation of the receptor tyrosine kinase Kit is required for the proliferation of melanoblasts in the mouse embryo. Dev. Biol. 192, 99–107.

Matera, I., Watkins-Chow, D.E., Loftus, S.K., Hou, L., Incao, A., Silver, D.L., Rivas, C., Elliott, E.C., Baxter, L.L., Pavan, W.J., 2008. A sensitized mutagenesis screen identifies Gli3 as a modifier of Sox10 neurocristopathy. Hum. Mol. Genet. 17, 2118–2131.

Michelle, L., Cloutier, A., Toutant, J., Shkreta, L., Thibault, P., Durand, M., Garneau, D., Gendron, D., Lapointe, E., Couture, S., Le Hir, H., Klinck, R., Elela, S.A., Prinos, P., Chabot, B., 2012. Proteins associated with the exon junction complex also control the alternative splicing of apoptotic regulators. Mol. Cell. Biol. 32, 954–967.

Miyamura, Y., Coelho, S.G., Wolber, R., Miller, S.A., Wakamatsu, K., Zmudzka, B.Z., Ito, S., Smuda, C., Passeron, T., Choi, W., Batzer, J., Yamaguchi, Y., Beer, J.Z., Hearing, V.J., 2007. Regulation of human skin pigmentation and responses to ultraviolet radiation. Pigm. Cell Res./Eur. Soc. Pigm. Cell Res. Int. Pigm. Cell Soc. 20, 2–13.

Nott, A., Le Hir, H., Moore, M.J., 2004. Splicing enhances translation in mammalian cells: an additional function of the exon junction complex. Genes Dev. 18, 210–222.

Palacios, I.M., Gatfield St, D., Johnston, D., Izaurralde, E., 2004. An eIF4AIII-containing complex required for mRNA localization and nonsense-mediated mRNA decay. Nature 427, 753–757.

Potterf, S.B., Mollaaghababa, R., Hou, L., Southard-Smith, E.M., Hornyak, T.J., Arnheiter, H., Pavan, W.J., 2001. Analysis of SOX10 function in neural crest-derived melanocyte development: SOX10-dependent transcriptional control of dopachrome tautomerase. Dev. Biol. 237, 245–257.

Prasad, M.K., Reed, X., Gorkin, D.U., Cronin, J.C., McAdow, A.R., Chain, K., Hodonsky, C.J., Jones, E.A., Svaren, J., Antonellis, A., Johnson, S.L., Loftus, S.K., Pavan, W.J., McCallion, A.S., 2011. SOX10 directly modulates ERBB3 transcription via an intronic neural crest enhancer. BMC Dev. Biol. 11, 40.

Rigel, D.S., 2010. Trends in dermatology: melanoma incidence. Arch. Dermatol. 146, 318.

Serbedzija, G.N., Bronner-Fraser, M., Fraser, S.E., 1992. Vital dye analysis of cranial neural crest cell migration in the mouse embryo. Development 116, 297–307.

Serbedzija, G.N., Bronner-Fraser, M., Fraser, S.E., 1994. Developmental potential of trunk neural crest cells in the mouse. Development 120, 1709–1718.

Silver, D.L., Hou, L., Pavan, W.J., 2006. The genetic regulation of pigment cell development. Adv. Exp. Med. Biol. 589, 155–169.

Silver, D.L., Hou, L., Somerville, R., Young, M.E., Apte, S.S., Pavan, W.J., 2008. The secreted metalloprotease ADAMTS20 is required for melanoblast survival. PLoS Genet. 4, e1000003.

Silver, D.L., Watkins-Chow, D.E., Schreck, K.C., Pierfelice, T.J., Larson, D.M., Burnetti, A.J., Liaw, H.J., Myung, K., Walsh, C.A., Gaiano, N., Pavan, W.J., 2010. The exon junction complex component Magoh controls brain size by regulating neural stem cell division. Nat. Neurosci. 13, 551–558.

Southard-Smith, E.M., Kos, L., Pavan, W.J., 1998. Sox10 mutation disrupts neural crest development in Dom Hirschsprung mouse model. Nat. Genet. 18, 60–64.

Wilkie, A.L., Jordan, S.A., Jackson, I.J., 2002. Neural crest progenitors of the melanocyte lineage: coat colour patterns revisited. Development 129, 3349–3357.

Yoshida, H., Kunisada, T., Kusakabe, M., Nishikawa, S., Nishikawa, S.I., 1996. Distinct stages of melanocyte differentiation revealed by anlaysis of nonuniform pigmentation patterns. Development 122, 1207–1214.